

Exploring the disk-jet connection in NGC 315

LUCA RICCI

**COLLABORATORS: B. BOCCARDI, E. NOKHRINA, M. PERUCHO,
N. MACDONALD, G. MATTIA, P. GRANDI, E. MADIKA**

AGNs - disk-jet connection

Virially hot and optically thin

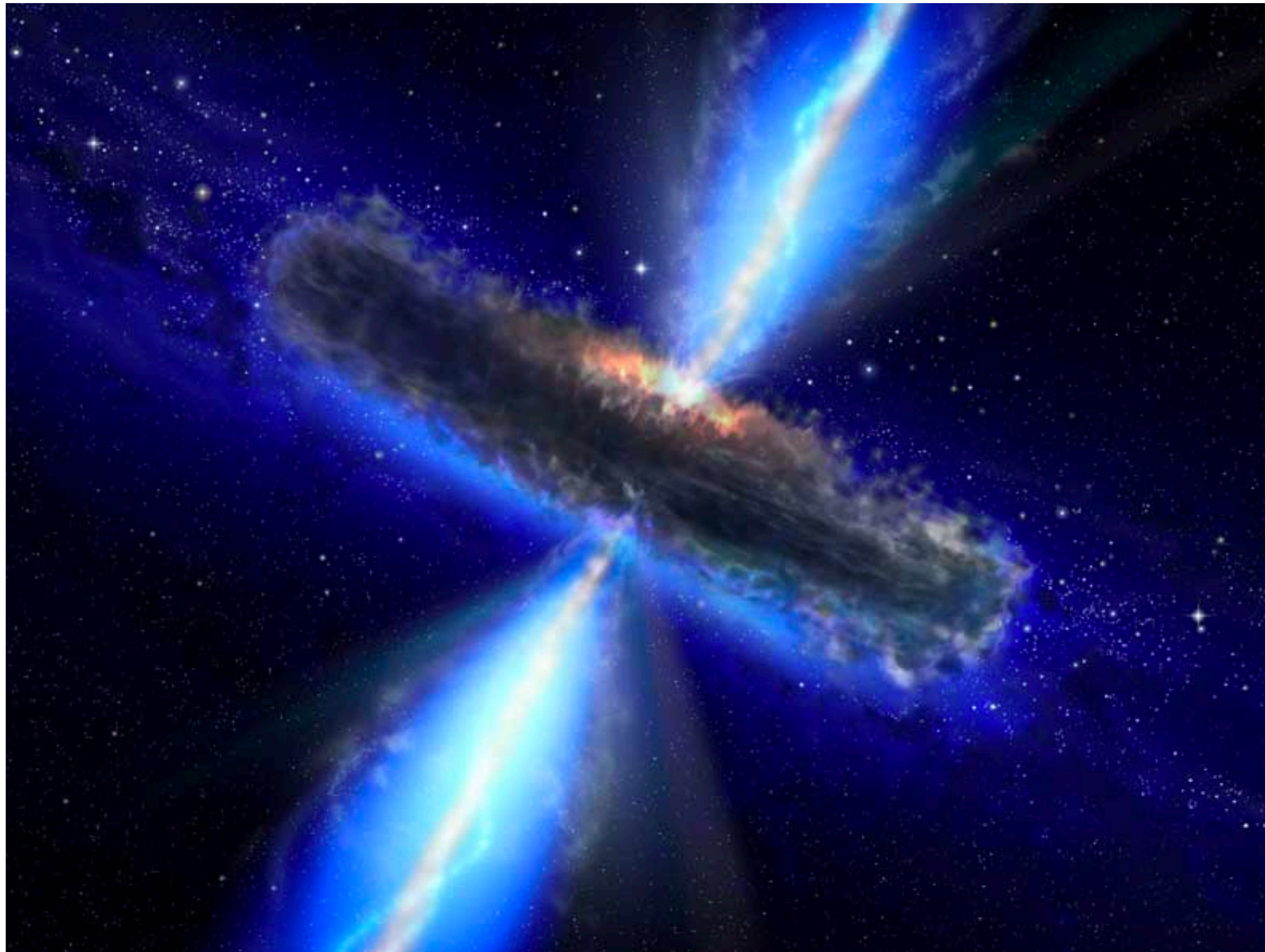
See the review
Yuan+, 2014



Hot accretion flows are able to eject the powerful relativistic jets we see in AGNs.

SANE (Standard And Normal Evolution)

MAD (Magnetically Arrested Disks)



Magnetically arrested disks (MAD)

A significant amount of poloidal magnetic flux is collected in the vicinity of the black hole

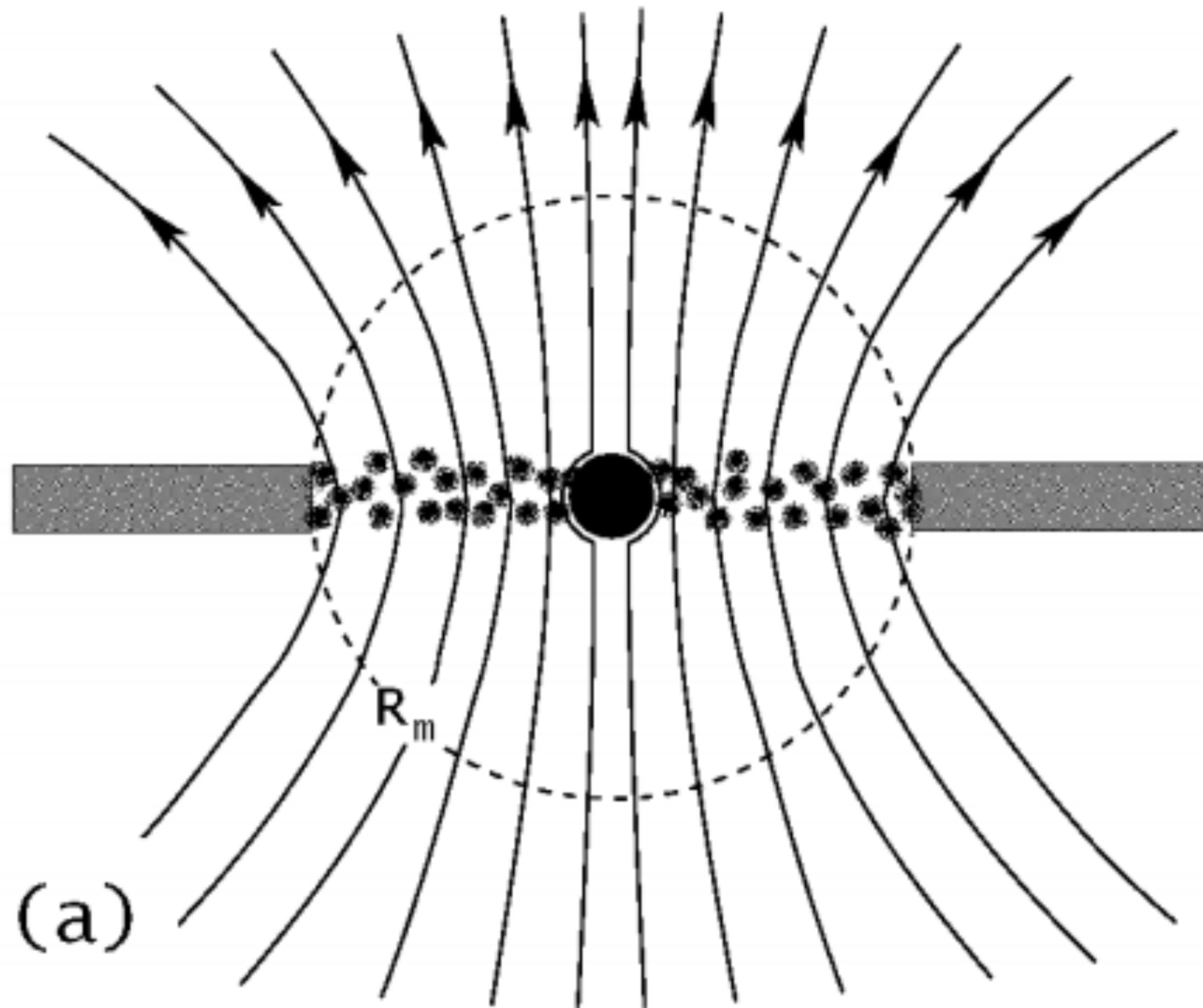


The accumulated magnetic poloidal field disrupts the accretion flow at the distance $R_m = r_m R_s$

- R_s Schwarzschild radius
- r_m magnetosphere in units of R_s
- R_m magnetosphere radius

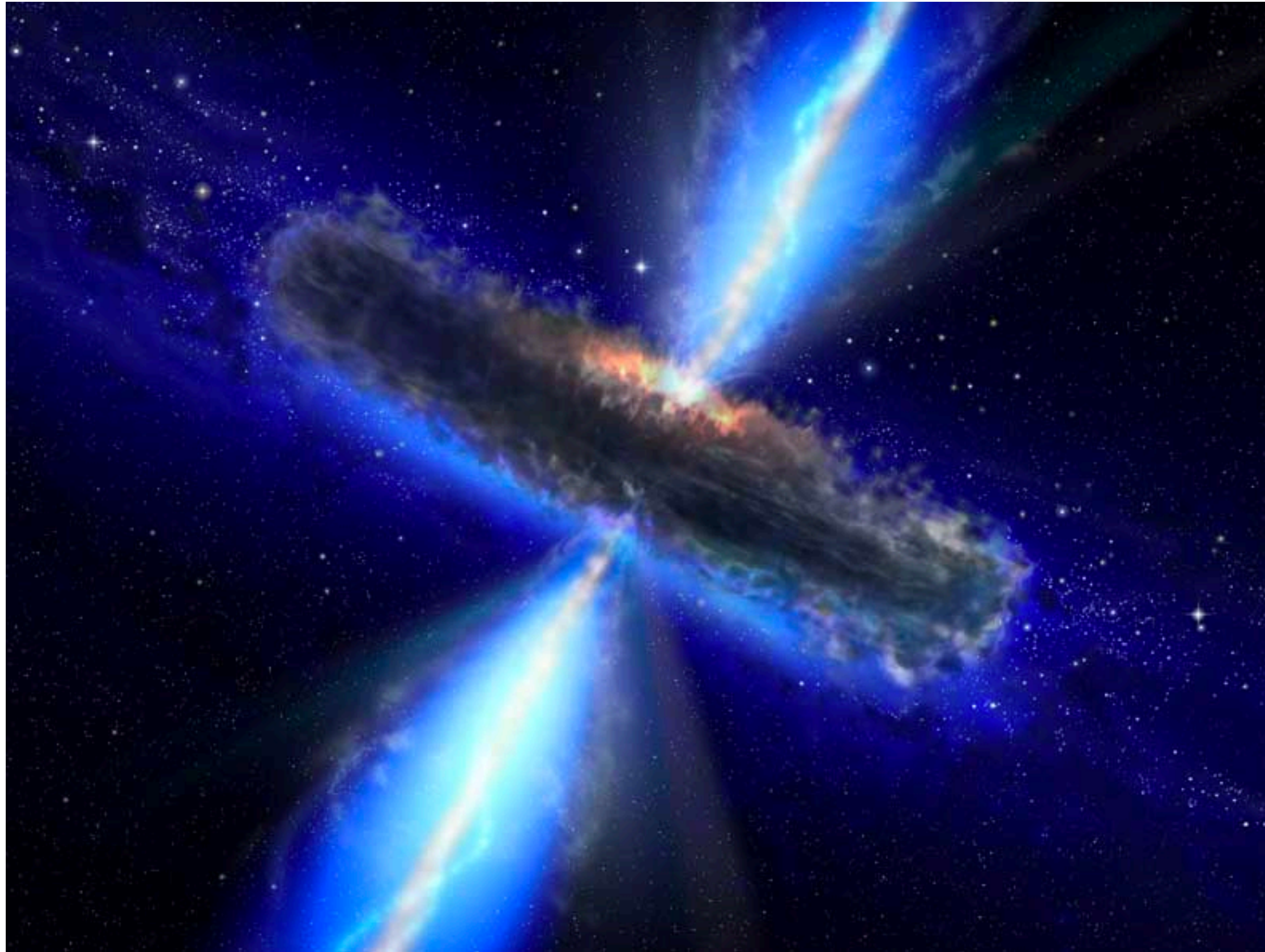


The flow breaks into blobs or streams and the gas goes towards the black hole



Confirmed in numerous simulation works (e.g. [McKinney+, 2012](#), [White+, 2019](#), [Narayan+, 2021](#))

AGNs - disk-jet connection

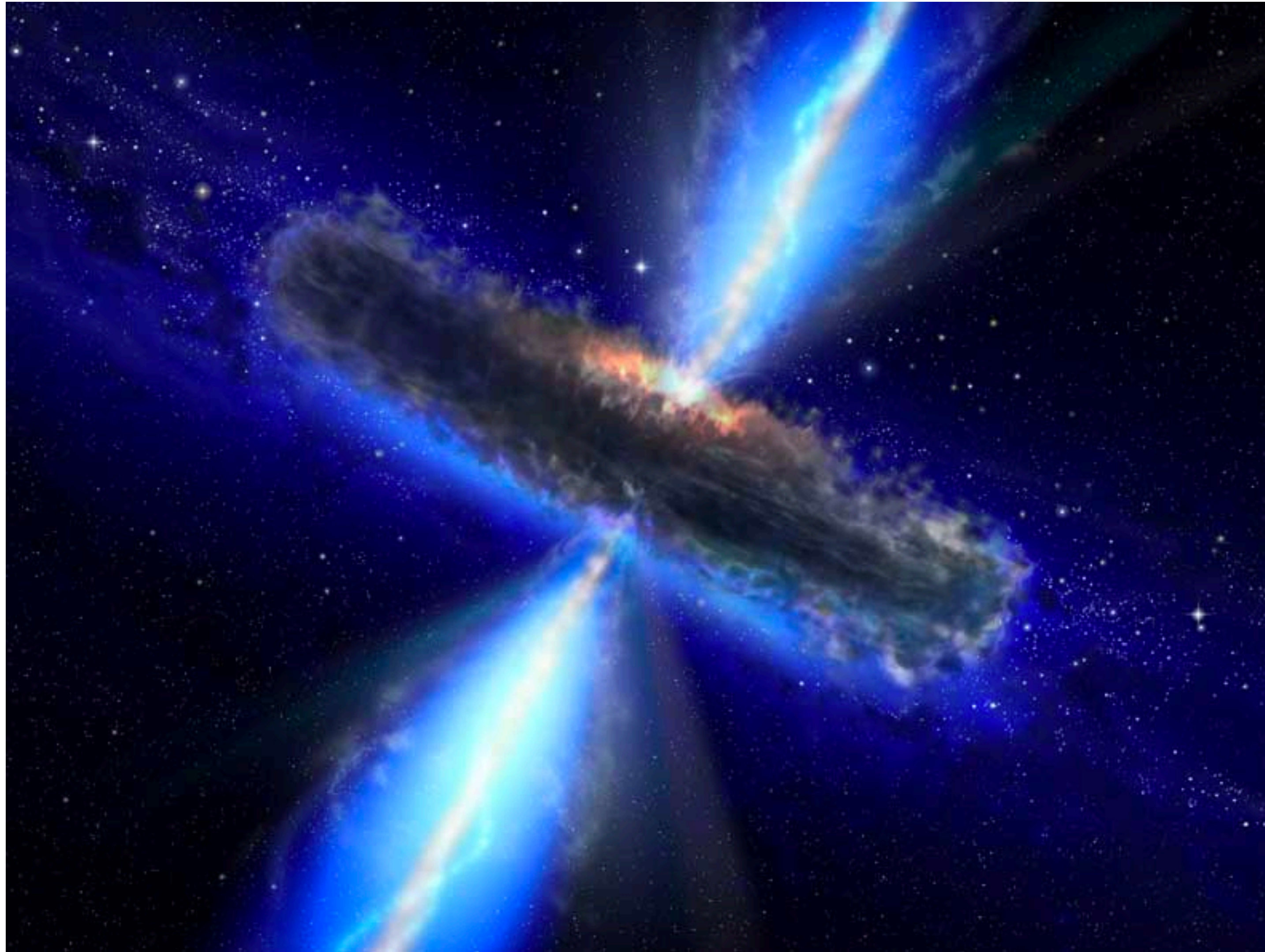


Hot accretion flows are able to eject the powerful relativistic jets we see in AGNs.

SANE (Standard And Normal Evolution)

MAD (Magnetically Arrested Disks)

AGNs - disk-jet connection



Hot accretion flows are able to eject the powerful relativistic jets we see in AGNs.

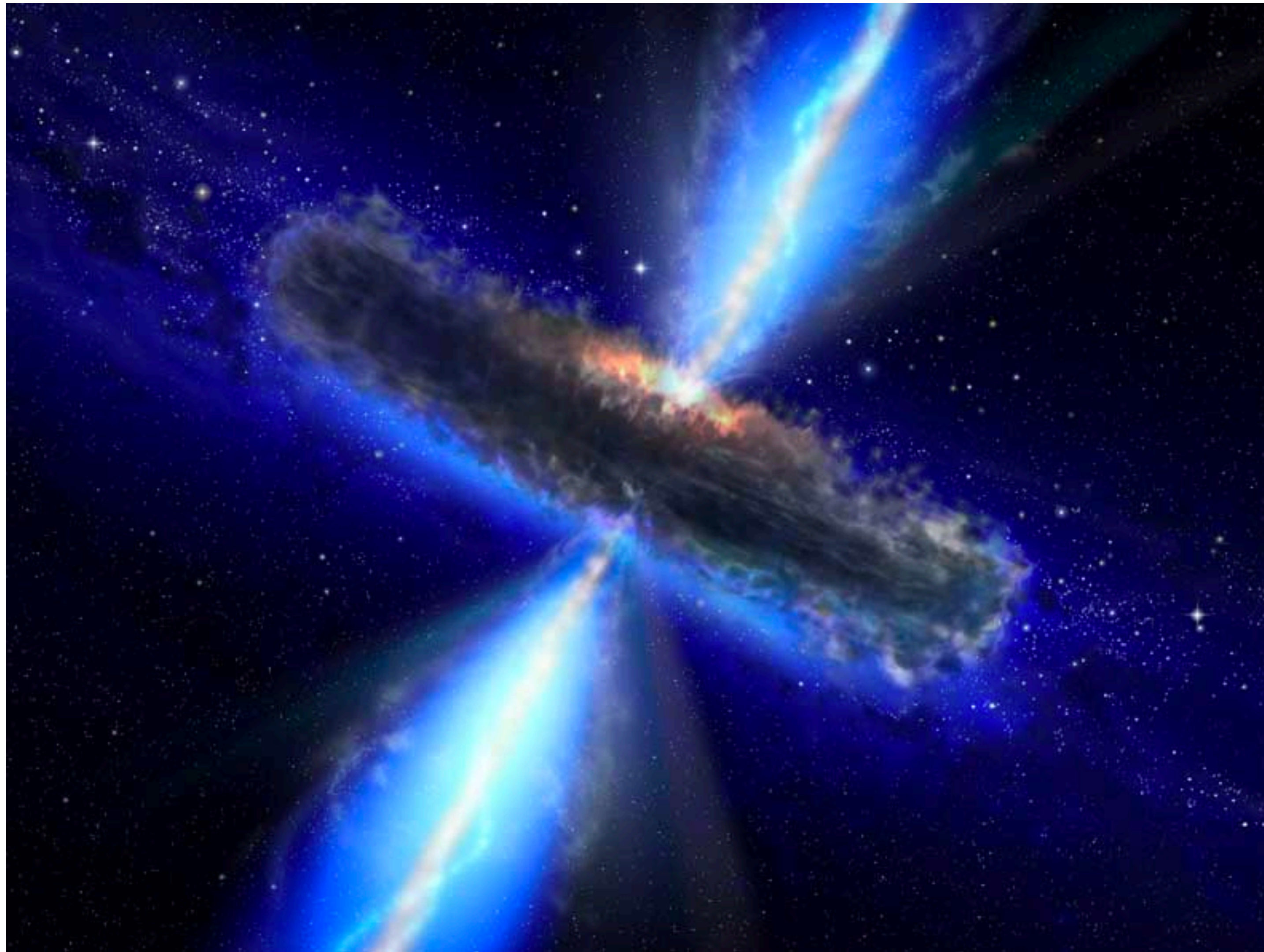
SANE (Standard And Normal Evolution)

MAD (Magnetically Arrested Disks)



Different magnetic field properties: in the accretion disk and...

AGNs - disk-jet connection



Hot accretion flows are able to eject the powerful relativistic jets we see in AGNs.

SANE (Standard And Normal Evolution)

MAD (Magnetically Arrested Disks)

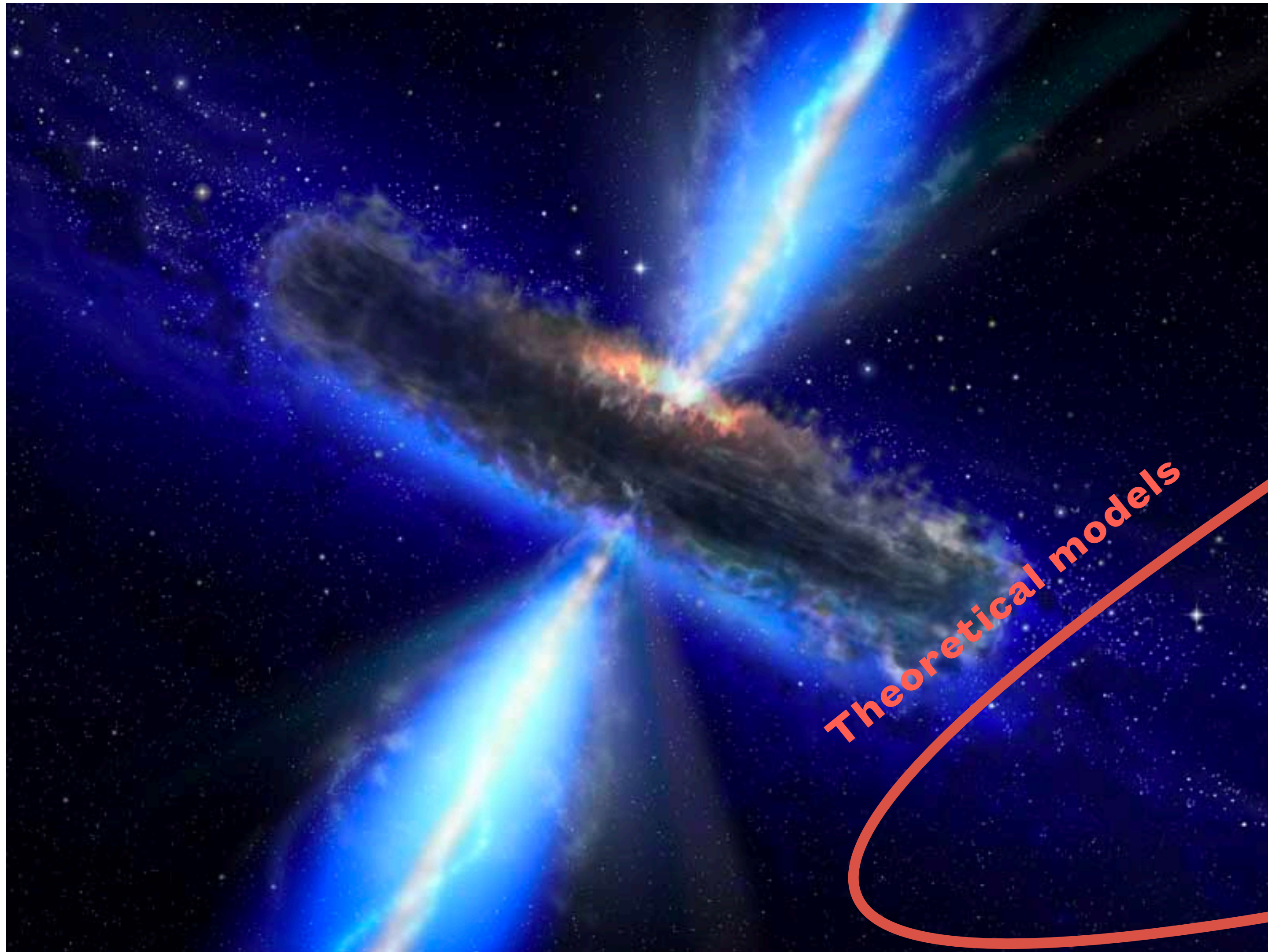


Different magnetic field properties: in the accretion disk and...



..in the jet → different jet observational properties

AGNs - disk-jet connection



Hot accretion flows are able to eject the powerful relativistic jets we see in AGNs.

SANE (Standard And Normal Evolution)

MAD (Magnetically Arrested Disks)



Different magnetic field properties: in the accretion disk and...



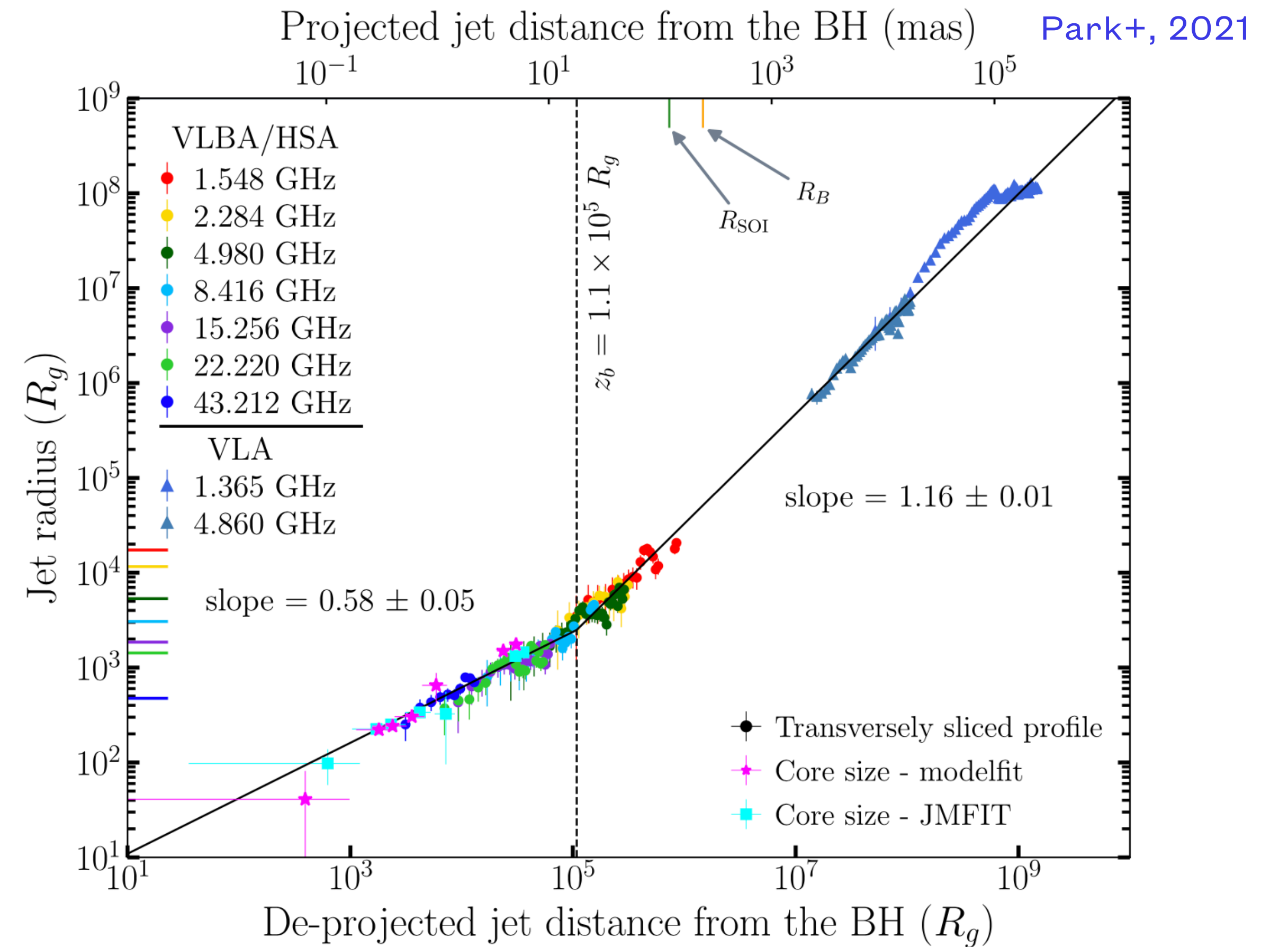
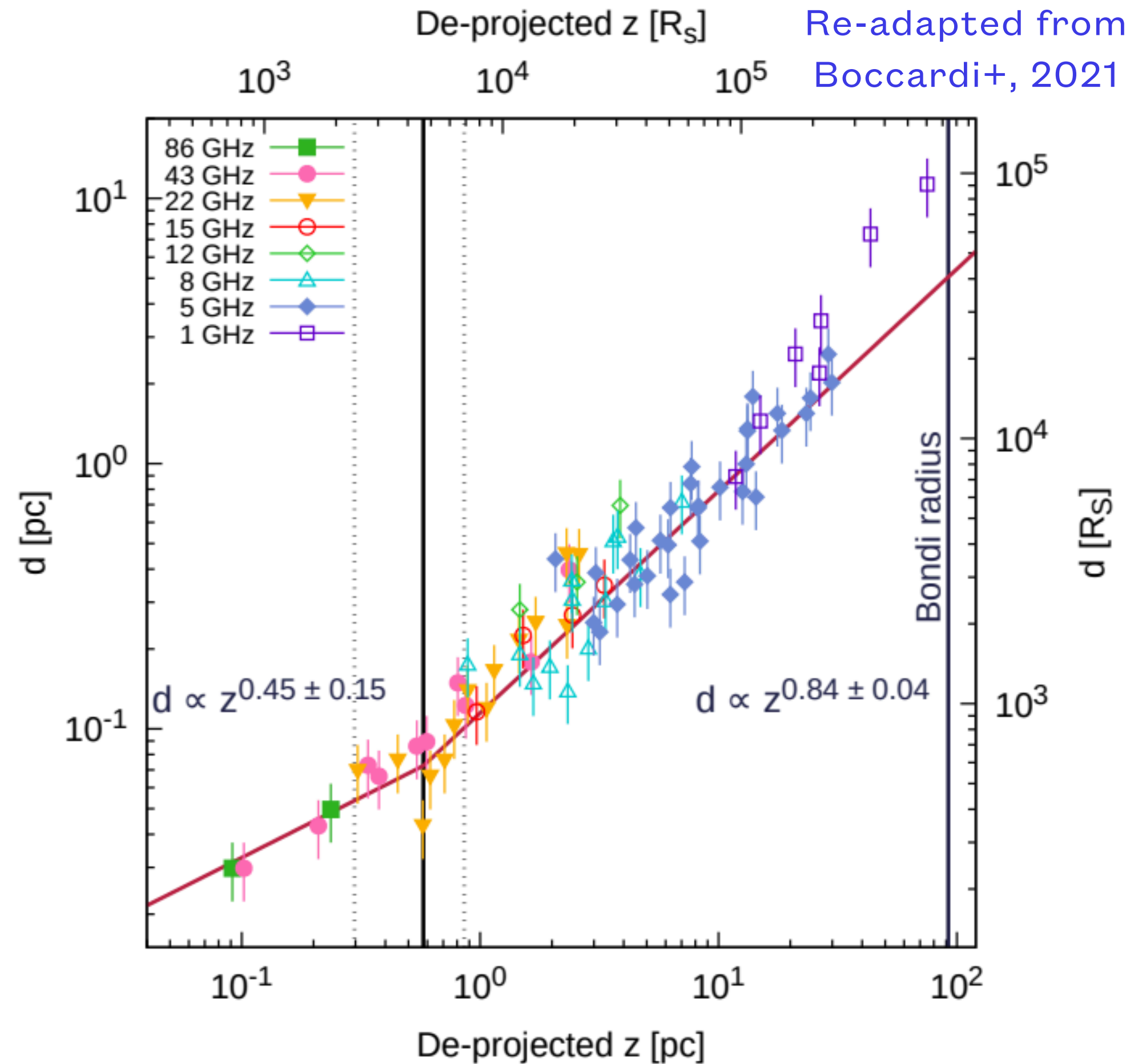
..in the jet → different jet observational properties

Theoretical models

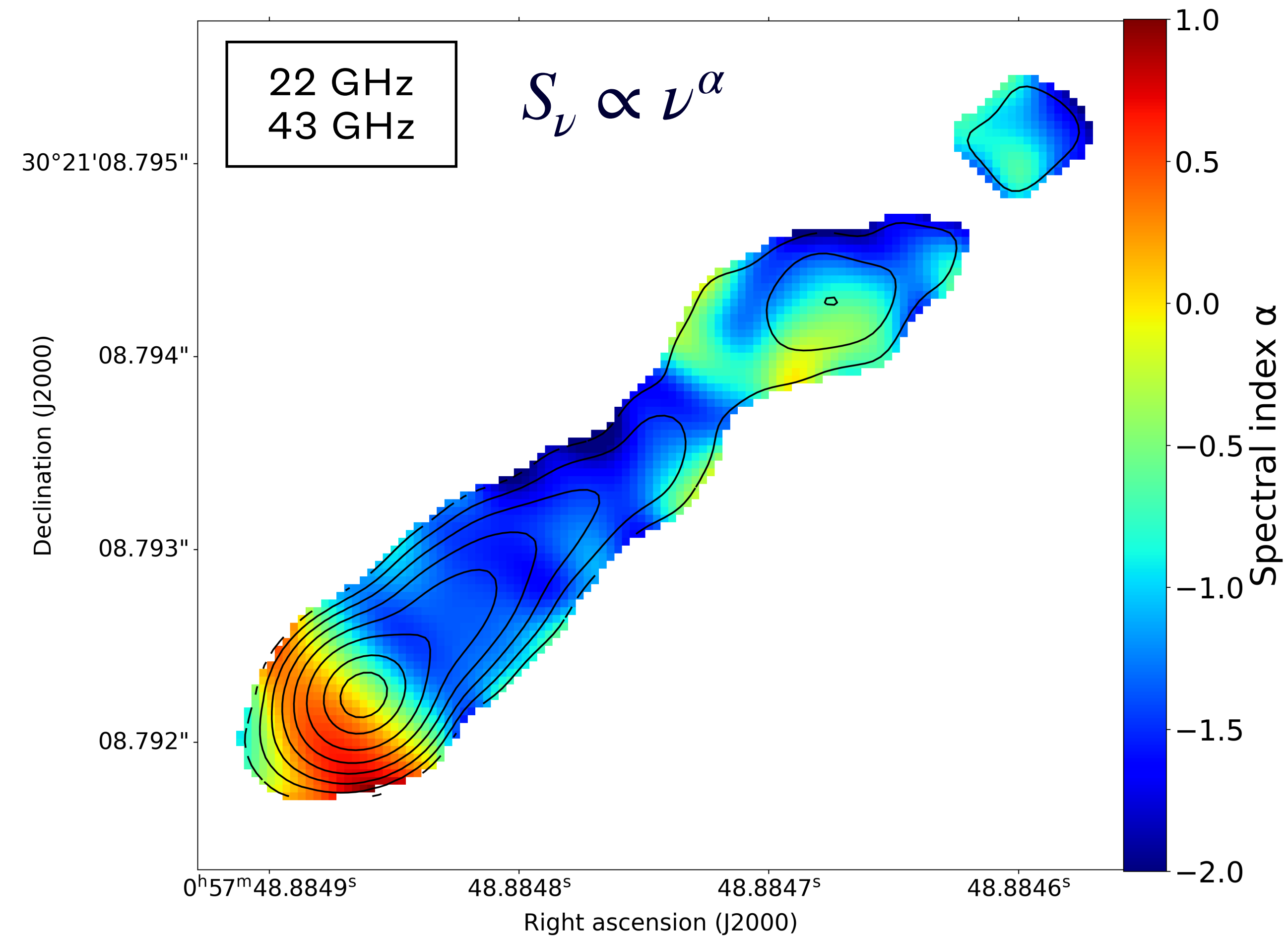
Why NGC 315?

In NGC 315 we can observe the **acceleration and collimation region**

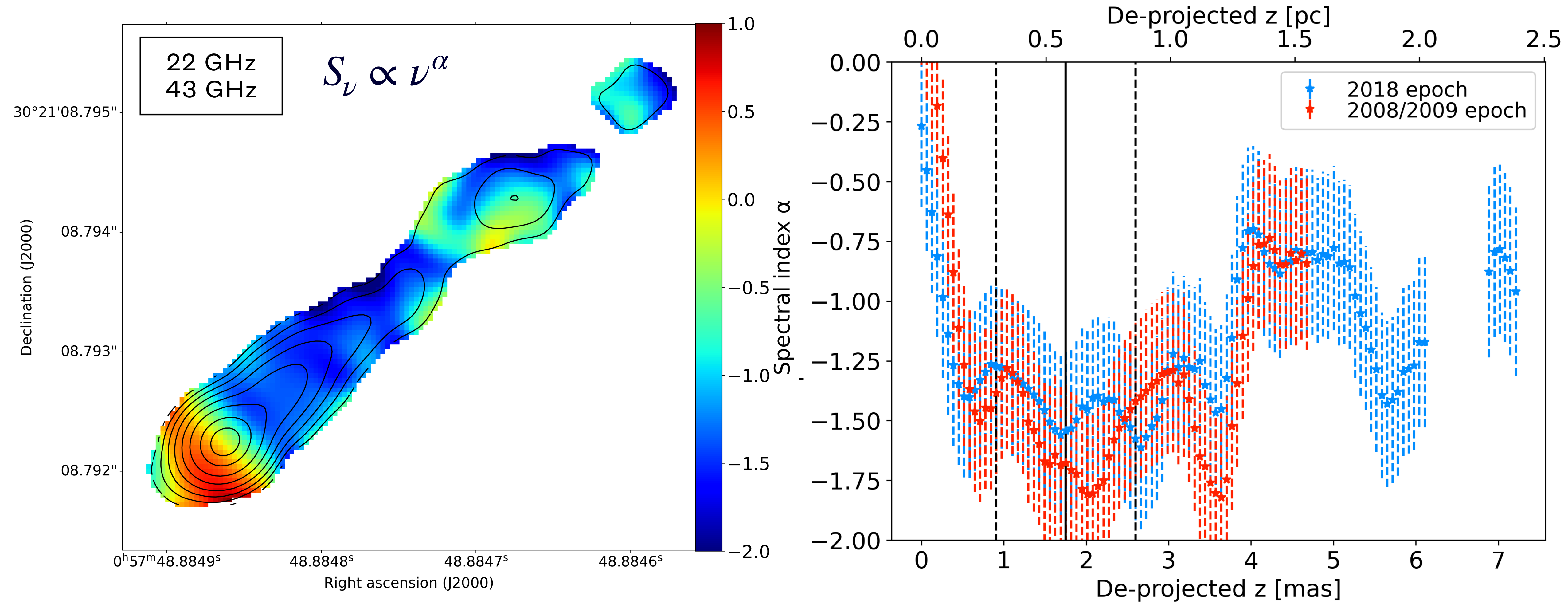
we will see it in a bit



Spectral analysis



Spectral analysis



In a distance range similar to the collimation region the spectral index shows very steep values \rightarrow synchrotron losses due to strong magnetic fields?

Jet speed

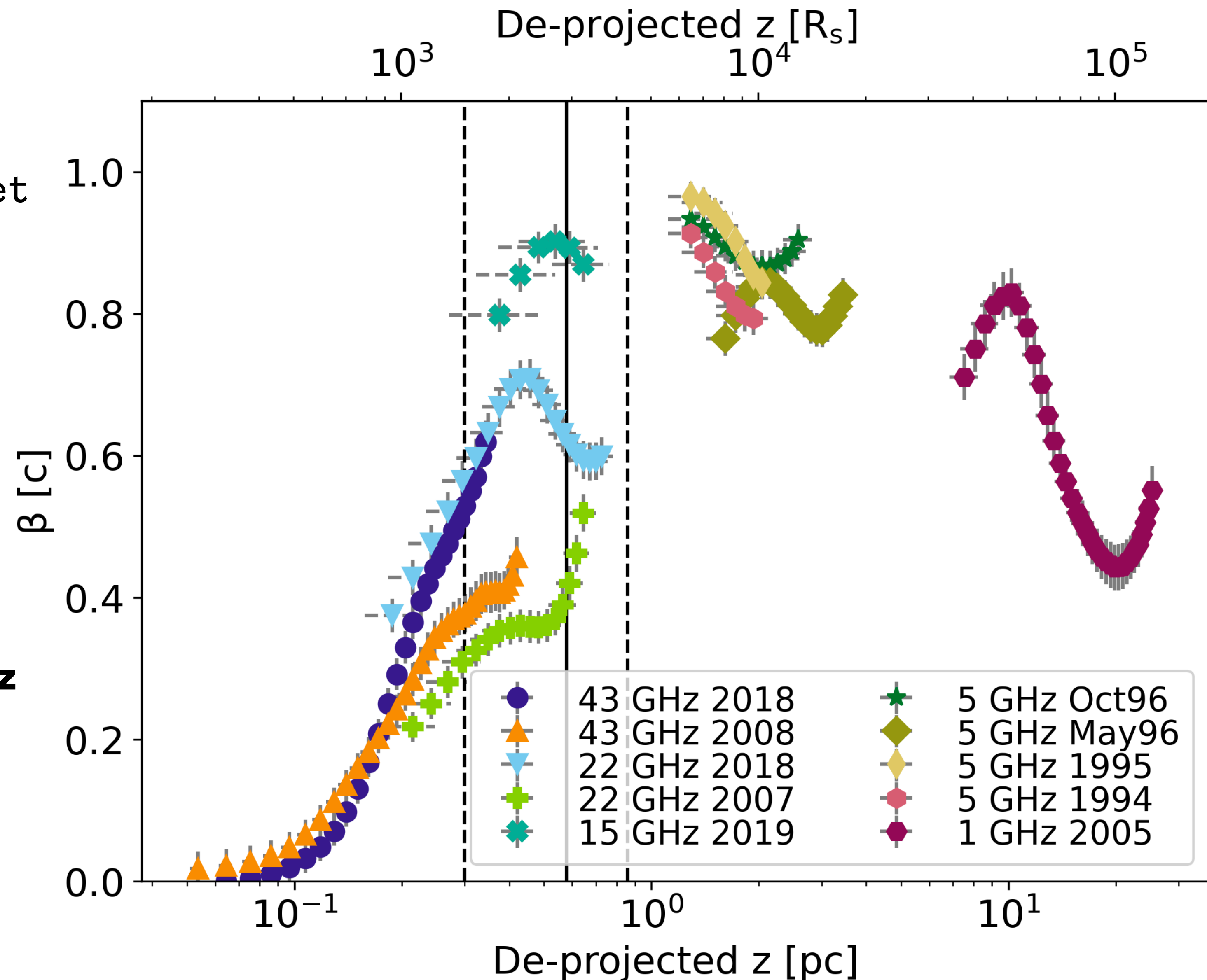
Jet to counter-jet intensity ratio

H_p: intrinsic symmetry between the jet and the counter-jet

$$\beta = \frac{1}{\cos(\theta)} \cdot \frac{R^{1/p} - 1}{R^{1/p} + 1}$$

$$p = 2 - \alpha \quad (S_\nu \propto \nu^\alpha)$$

The maps are aligned on the 43 GHz core (Boccardi+, 2021)



Jet speed

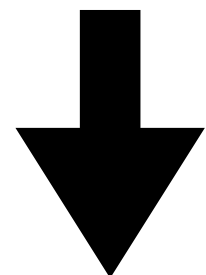
Jet to counter-jet intensity ratio

H_p: intrinsic symmetry between the jet and the counter-jet

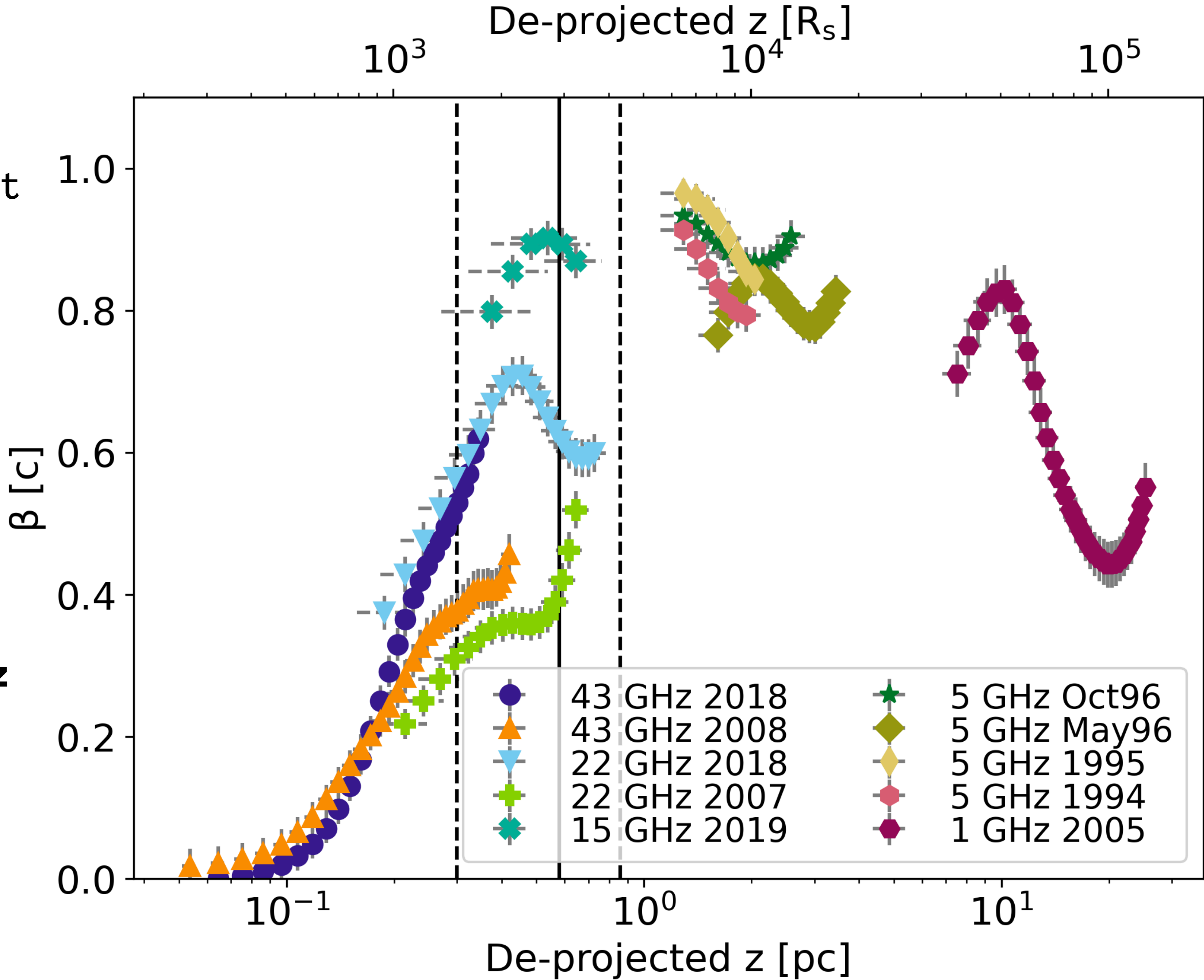
$$\beta = \frac{1}{\cos(\theta)} \cdot \frac{R^{1/p} - 1}{R^{1/p} + 1}$$

$$p = 2 - \alpha \quad (S_\nu \propto \nu^\alpha)$$

The maps are aligned on the 43 GHz core (Boccardi+, 2021)

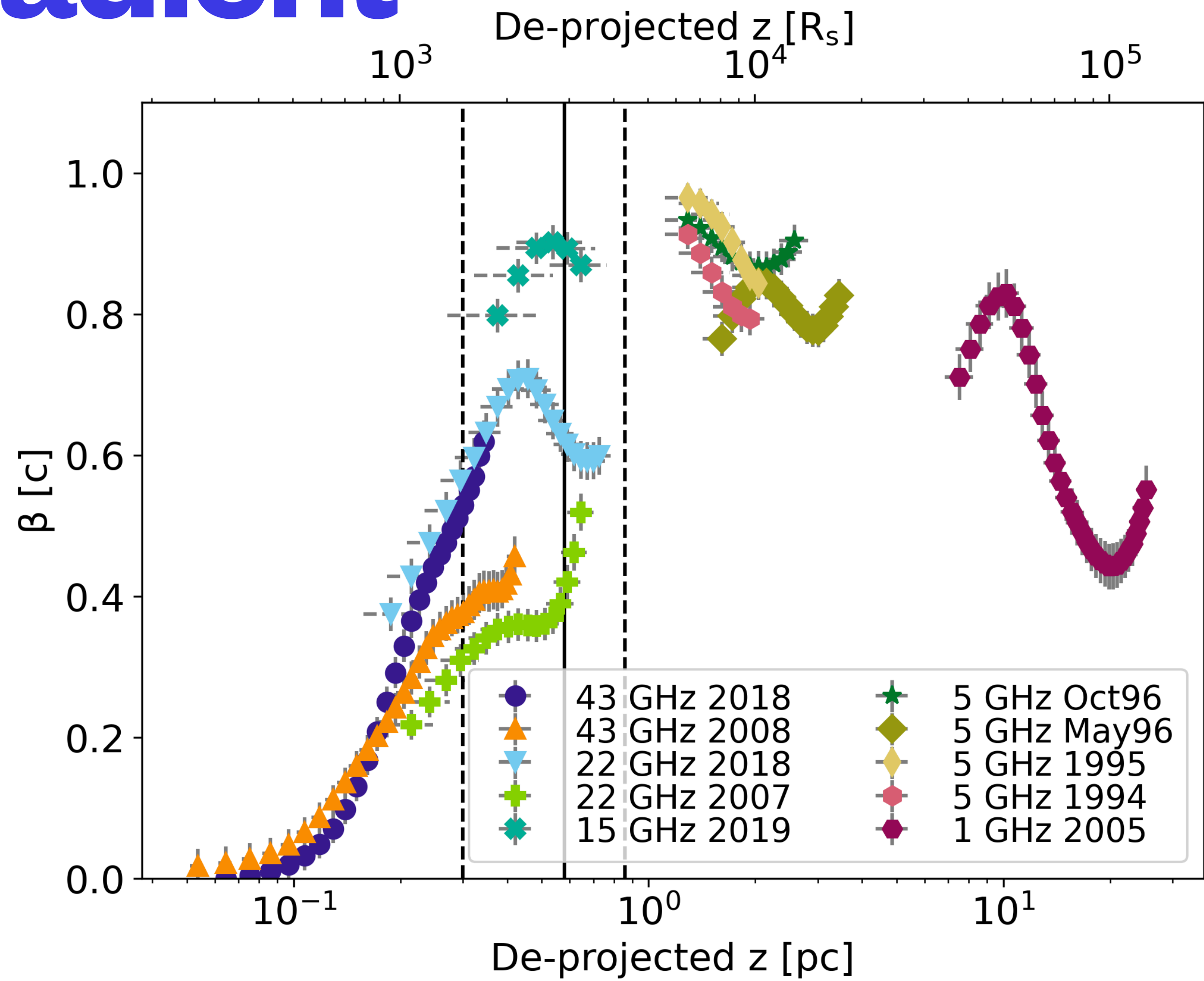


magnetically driven acceleration



Jet acceleration gradient

$$f(z) = A + B \tanh(ar - b)$$

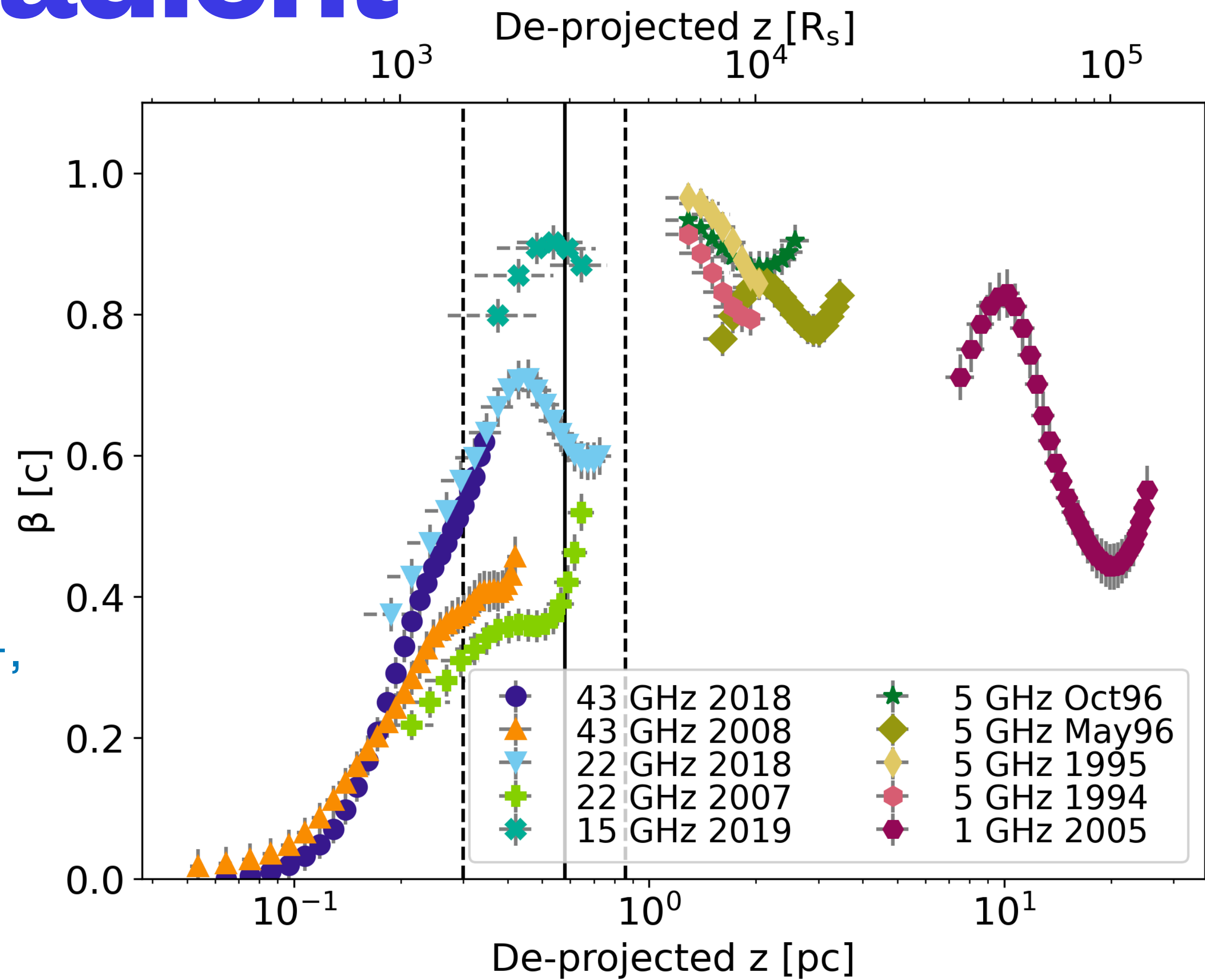


Jet acceleration gradient

$$f(z) = A + B \tanh(ar - b)$$

- $f(0) = 1$
- $f(\infty) = \Gamma_{\max}$
- $\delta\Gamma/\delta r < R_L^{-1}$
- $\Gamma = \Gamma_{\max}/2$ @ $r \sim R_L \Gamma_{\max}/2\rho$

MHD conditions (Beskin+, 2006, Tchekhovskoy+, 2009, Lyubarsky+, 2009; Nakamura+, 2018)



Jet acceleration gradient

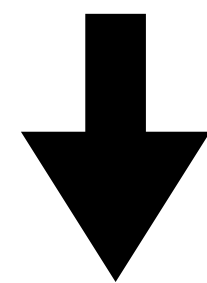
$$f(z) = A + B \tanh(ar - b)$$

- $f(0) = 1$
- $f(\infty) = \Gamma_{\max}$

- $\delta\Gamma/\delta r < R_L^{-1}$

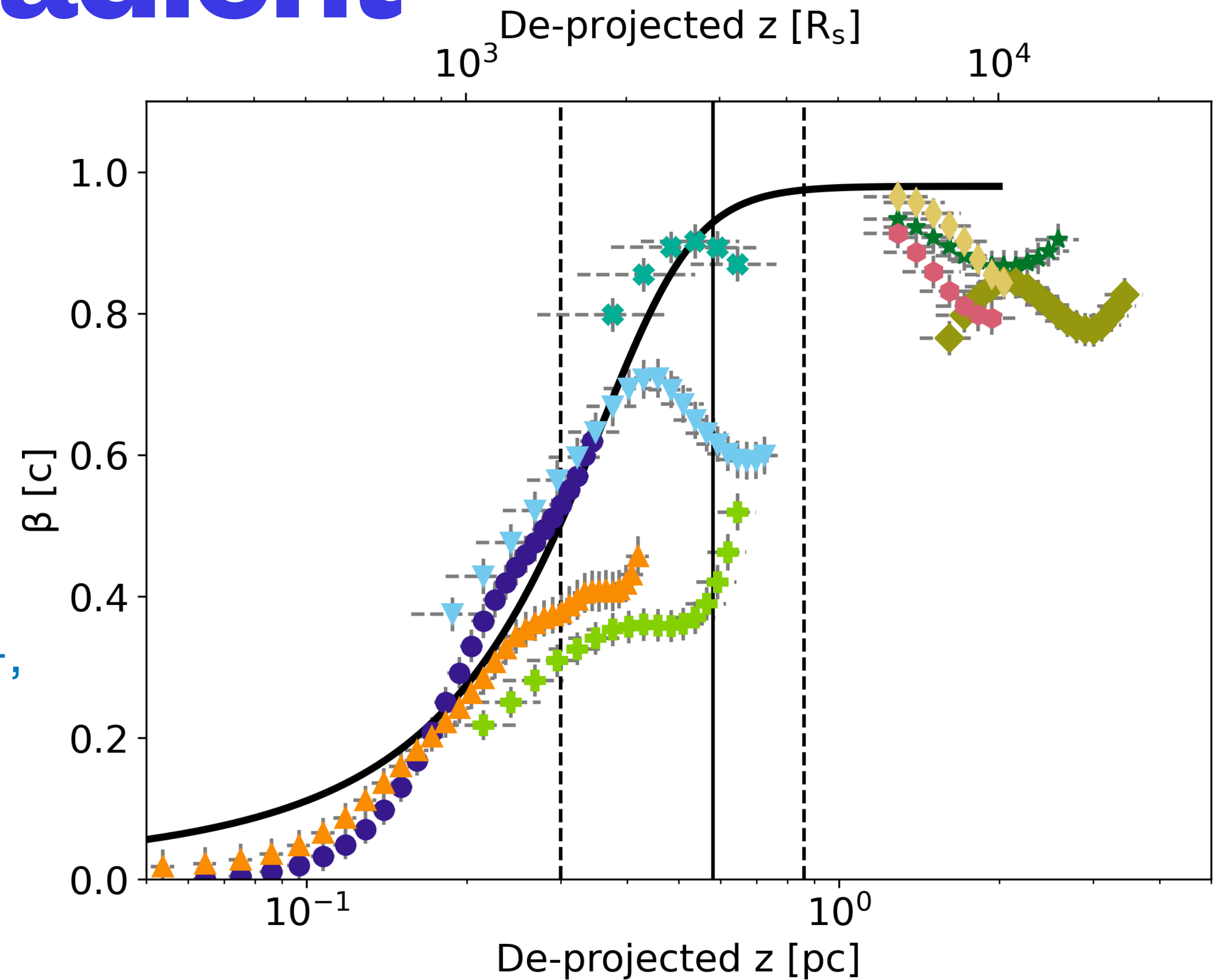
- $\Gamma = \Gamma_{\max}/2 @ r \sim R_L \Gamma_{\max}/2\rho$

MHD conditions (Beskin+, 2006, Tchekhovskoy+, 2009, Lyubarsky+, 2009; Nakamura+, 2018)



$$\Gamma(z) = \frac{\Gamma_{\max} + 1}{2} + \frac{\Gamma_{\max} - 1}{2} \tanh\left(\frac{z}{R_L} \frac{2}{\Gamma_{\max} - 1} - \frac{\Gamma_{\max}}{\rho(\Gamma_{\max} - 1)}\right)$$

Theoretically reconciled with a magnetically driven acceleration



Nuclear properties

- **Black hole spin** (Nokhrina+ (2019,2020))

$$a_* = \frac{8(r_g/R_L)}{1 + 16(r_g/R_L)^2} \gtrsim 0.72$$

Nuclear properties

- **Black hole spin** (Nokhrina+ (2019,2020))

$$a_* = \frac{8(r_g/R_L)}{1 + 16(r_g/R_L)^2} \gtrsim 0.72$$

- **Magnetic flux threading the accretion disk** (Nokhrina+ (2019,2020))

$$\Phi_N = (1.1 \pm 0.8) \times 10^{33} \text{ G cm}^2$$



obs + model

Nuclear properties

- **Black hole spin** (Nokhrina+ (2019,2020))

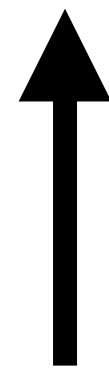
$$a_* = \frac{8(r_g/R_L)}{1 + 16(r_g/R_L)^2} \gtrsim 0.72$$

- **Magnetic flux threading the accretion disk** (Nokhrina+ (2019,2020) and Zamaninasab+, 2014)

$$\Phi_N = (1.1 \pm 0.8) \times 10^{33} \text{ G cm}^2 \quad \sim \quad \Phi^{\text{exp}} = (1.4 \pm 0.3) \times 10^{33} \text{ G cm}^2$$



obs + model



expected



First hint for an established MAD

Magnetic field based on the core shift

- Conical geometry (Lobanov, 1998 and Hirotani, 2005)

- Case 0)
$$B_1 = 0.025 \left(\frac{\Omega_{rv}^3 (1 + Z)^2}{\delta^2 \phi \sin^2 \theta} \right)^{1/4} \text{ G}$$

Magnetic field based on the core shift

- Conical geometry (Lobanov, 1998 and Hirotani, 2005)

- Case 0)
$$B_1 = 0.025 \left(\frac{\Omega_{r\nu}^3 (1+Z)^2}{\delta^2 \phi \sin^2 \theta} \right)^{1/4} \text{ G}$$

where:
$$\Omega_{r\nu} = 4.85 \times 10^{-9} \frac{\Delta r_{\text{mas}} D_L}{(1+z)^2} \left(\frac{\nu_1^{1/k_r} \nu_2^{1/k_r}}{\nu_2^{1/k_r} - \nu_1^{1/k_r}} \right) \text{ pc GHz}$$

Core shift



Magnetic field based on the core shift

- Conical geometry ([Lobanov, 1998](#) and [Hirotani, 2005](#))

- Case 0)
$$B_1 = 0.025 \left(\frac{\Omega_{r\nu}^3 (1 + Z)^2}{\delta^2 \phi \sin^2 \theta} \right)^{1/4} \text{ G}$$

- Quasi-parabolic geometry and accelerating jet ([Ricci+, 2022arXiv220612193R, A&A in press](#))

- Case A) $\theta \sim \Gamma^{-1}$
$$B_z = 0.025 \left(\frac{\Omega_{r\nu}^{6\psi} (1 + Z)^2}{z^{6\psi} r_z \delta^2 \sin^{6\psi-1} \theta} \right)^{1/4} \text{ G}$$

- Case B) $\theta \lesssim \Gamma^{-1}$
$$B_z = 0.018 \left(\frac{\Omega_{r\nu}^{4\psi} (1 + Z)^2}{z^{4\psi} r_z \sin^{4\psi-1} \theta} \left(\frac{R_L}{r_z} \right)^2 \right)^{1/4} \text{ G} \quad z \propto r^\psi$$

- Case C) $\theta \gtrsim \Gamma^{-1}$
$$B_z = 0.025 \left(\frac{\Omega_{r\nu}^{8\psi} (1 + Z)^2 (1 - \cos \theta)^2}{z^{8\psi} r_z \sin^{8\psi-1} \theta} \left(\frac{R_L}{r_z} \right)^2 \right) \text{ G}$$

Magnetic field based on the core shift

- Conical geometry ([Lobanov, 1998](#) and [Hirotani, 2005](#))

- Case 0)
$$B_1 = 0.025 \left(\frac{\Omega_{r\nu}^3 (1 + Z)^2}{\delta^2 \phi \sin^2 \theta} \right)^{1/4} \text{ G}$$

$$B_1 = 0.13 \pm 0.02 \text{ G}$$

- Quasi-parabolic geometry and accelerating jet ([Ricci+, 2022arXiv220612193R, A&A in press](#))

$$z_{\text{br}} = 0.58 \text{ pc}$$

- Case A) $\theta \sim \Gamma^{-1}$
$$B_z = 0.025 \left(\frac{\Omega_{r\nu}^{6\psi} (1 + Z)^2}{z^{6\psi} r_z \delta^2 \sin^{6\psi-1} \theta} \right)^{1/4} \text{ G}$$

$$B_{z_{\text{br}}} = 0.18 \pm 0.06 \text{ G}$$

- Case B) $\theta \lesssim \Gamma^{-1}$
$$B_z = 0.018 \left(\frac{\Omega_{r\nu}^{4\psi} (1 + Z)^2 \left(\frac{R_L}{r_z} \right)^2}{z^{4\psi} r_z \sin^{4\psi-1} \theta} \right)^{1/4} \text{ G}$$

$$B_{z_{\text{br}}} = 0.013 \pm 0.003 \text{ G}$$

- Case C) $\theta \gtrsim \Gamma^{-1}$
$$B_z = 0.025 \left(\frac{\Omega_{r\nu}^{8\psi} (1 + Z)^2 (1 - \cos \theta)^2 \left(\frac{R_L}{r_z} \right)^2}{z^{8\psi} r_z \sin^{8\psi-1} \theta} \right) \text{ G}$$

Accretion disk magnetic field

Method 1: core shift

- Case 0) $B_1 = 0.13 \pm 0.02 \text{ G}$
- Case A) $B_{z_{\text{br}}} = 0.18 \pm 0.06 \text{ G}$
- Case B) $B_{z_{\text{br}}} = 0.013 \pm 0.003 \text{ G}$

Accretion disk magnetic field

Method 1: core shift

- Case 0) $B_1 = 0.13 \pm 0.02$ G In an accelerating jet
- Case A) $B_{z_{br}} = 0.18 \pm 0.06$ G
- Case B) $B_{z_{br}} = 0.013 \pm 0.003$ G



$$B(z) = B_0 \left(\frac{z_0}{z} \right)^{2\psi}$$



$$\psi \sim 0.5$$

**True for toroidal
and poloidal
dominated fields in
an accelerating jet**

$$B(z) \propto z^{-1}$$

Accretion disk magnetic field

Method 1: core shift

- Case 0) $B_1 = 0.13 \pm 0.02 \text{ G}$
- Case A) $B_{z_{\text{br}}} = 0.18 \pm 0.06 \text{ G}$
- Case B) $B_{z_{\text{br}}} = 0.013 \pm 0.003 \text{ G}$

Method 2: poloidal field strength

$$B_p = \Phi_N / (\pi r^2)$$

Accretion disk magnetic field

Method 1: core shift

- Case 0) $B_1 = 0.13 \pm 0.02 \text{ G}$
- Case A) $B_{z_{\text{br}}} = 0.18 \pm 0.06 \text{ G}$
- Case B) $B_{z_{\text{br}}} = 0.013 \pm 0.003 \text{ G}$

Method 2: poloidal field strength

$$B_p = \Phi_N / (\pi r^2)$$

Saturation field strengths (MAD scenario)

$$F_B = F_G$$

Accretion disk magnetic field

Method 1: core shift

- Case 0) $B_1 = 0.13 \pm 0.02$ G
- Case A) $B_{z_{br}} = 0.18 \pm 0.06$ G
- Case B) $B_{z_{br}} = 0.013 \pm 0.003$ G

Method 2: poloidal field strength

$$B_p = \Phi_N / (\pi r^2)$$

Saturation field strengths (MAD scenario)

$$F_B = F_G \longrightarrow B_{\text{MAD}} = \left(\frac{2GM_{\text{BH}}\dot{M}}{3r^3v_r h/r} \right)^{1/2} \text{ G}$$

magnetosphere radius

$$r_m \in [0.6, 5.3] R_S$$

Accretion disk magnetic field

Method 1: core shift

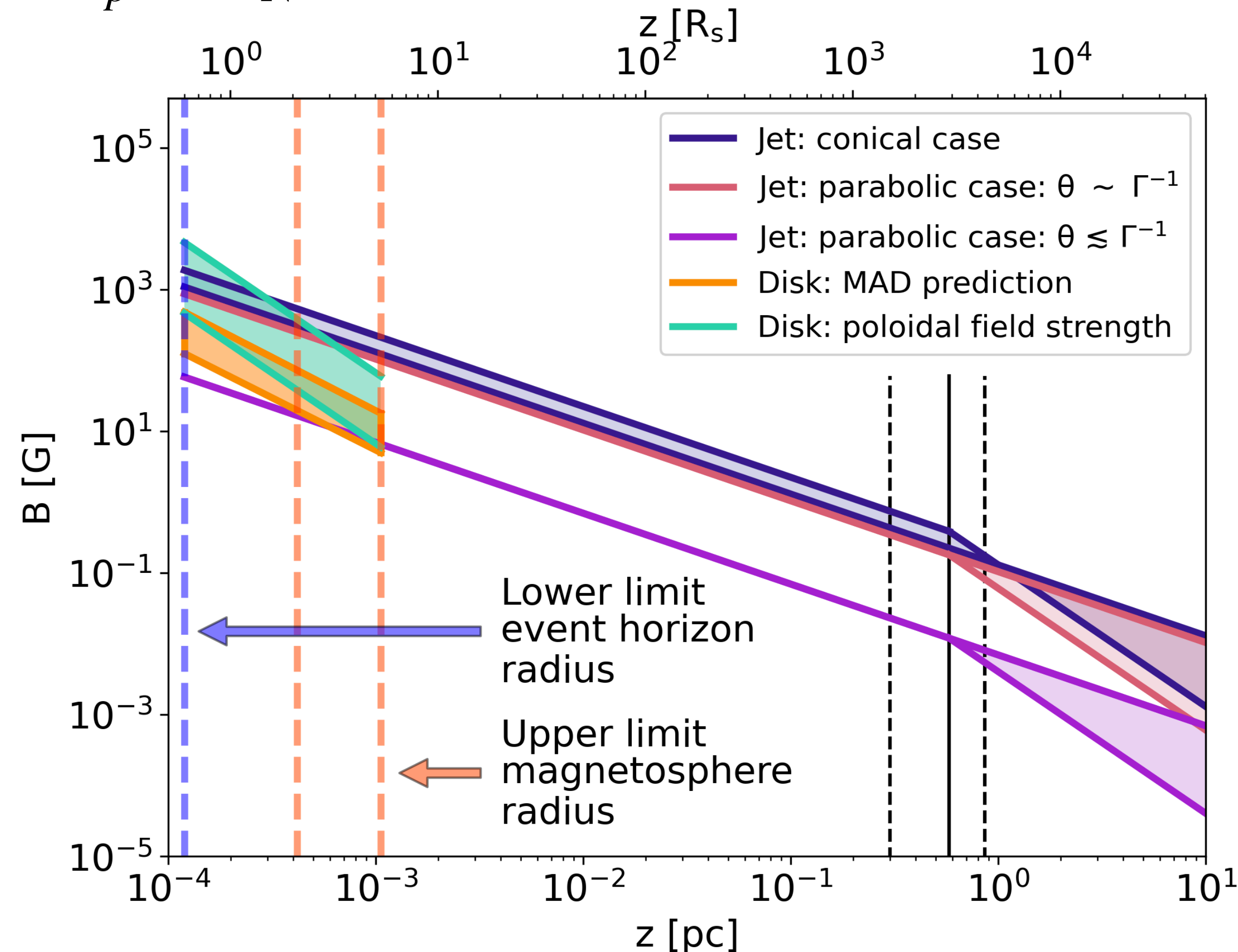
- Case 0) $B_1 = 0.13 \pm 0.02$ G
- Case A) $B_{z_{br}} = 0.18 \pm 0.06$ G
- Case B) $B_{z_{br}} = 0.013 \pm 0.003$ G

Saturation field strengths (MAD scenario)

$$F_B = F_G \longrightarrow B_{\text{MAD}} = \left(\frac{2GM_{\text{BH}}\dot{M}}{3r^3v_r h/r} \right)^{1/2} \text{ G}$$

Method 2: poloidal field strength

$$B_p = \Phi_N / (\pi r^2)$$



Accretion disk magnetic field

Method 1: core shift

- Case 0) $B_1 = 0.13 \pm 0.02$ G
- Case A) $B_{z_{br}} = 0.18 \pm 0.06$ G
- Case B) $B_{z_{br}} = 0.013 \pm 0.003$ G

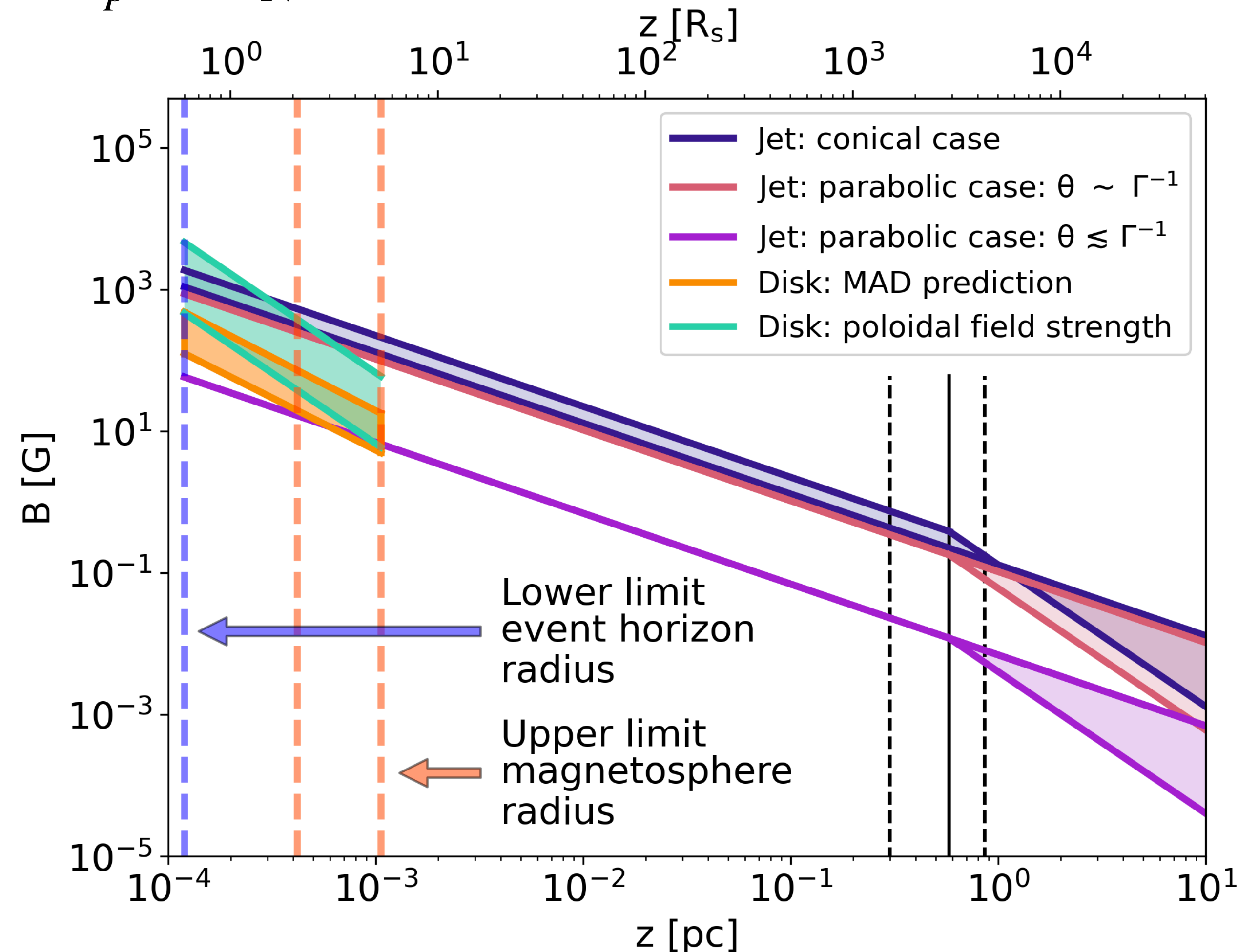
Saturation field strengths (MAD scenario)

$$F_B = F_G \longrightarrow B_{\text{MAD}} = \left(\frac{2GM_{\text{BH}}\dot{M}}{3r^3v_r h/r} \right)^{1/2} \text{ G}$$

Second hint for an established MAD

Method 2: poloidal field strength

$$B_p = \Phi_N / (\pi r^2)$$



Conclusions

- The collimation and acceleration scales are co-spatial —> it suggests the jet to consist of a **cold outflow in which the acceleration is mainly driven by the conversion of magnetic energy into kinetic energy of the bulk** (Komissarov+, 2007; Tchekhovskoy+, 2008; Lyubarsky+,2009). Following this, we modeled the jet acceleration in the context of MHD theories;
- We present a new formalism to compute the magnetic field from the core shift in a quasi-parabolic, accelerating jet. The extrapolated strengths are consistent with both the poloidal field values obtained from the magnetic disk flux and the needed saturation field strengths to form a MAD.
- Our analysis and modeling is compatible with a **fast-rotating black hole** surrounded by an **accretion disk that has reached a magnetically arrested state.**

Backup slide - Magnetic field extrapolation

$$B_\varphi = B'_\varphi / \Gamma \quad \text{Toroidal field} \quad B_z \quad \text{Estimated field}$$

$$B_p = B'_p \quad \text{Poloidal field}$$

$$B'_\varphi = B'_p r / R_L \quad \rightarrow \text{MHD relation for a relativistic flow}$$

The toroidal component dominates in the core region

$$B_g = B'_p \left(\frac{r}{r_g} \right)^2 = B_\varphi \Gamma R_L / r \left(\frac{r}{r_g} \right)^2 \quad \rightarrow \text{effective acceleration region} \quad \rightarrow B_g = B_z \left(\frac{z}{z_g} \right)^{2\psi}$$

$\Gamma \frac{R_L}{r} \sim 1$ and $r \propto z^\psi$

The poloidal component dominates in the core region

$$B_g = B'_p \left(\frac{r}{r_g} \right)^2 = B_p \left(\frac{r}{r_g} \right)^2 = B_z \left(\frac{z}{z_g} \right)^{2\psi}$$